The gaseous products characterization of the pyrolysis process of various agricultural residues using TGA–DSC–MS techniques

Bojan Janković[1] · Nebojša Manić[2] · Dragoslava Stojiljković[2]

Abstract

Slow pyrolysis characteristics of agricultural residue feedstocks (corn brakes, wheat straw, and hazelnut shell) were investigated by simultaneous thermal analysis (STA–TG–DTG–DSC), coupled with mass spectrometry (MS). Thermal decomposition of agricultural residues was divided into three stages, corresponding to removal of water, devolatilization, and formation of bio-char. It was found that differences in thermal behavior of samples are due to differences in their composition. The MS results showed that H_2, CH_4, H_2O, CO_2 (C_3H_8), CO, and C_2H_6 were the main gaseous products released during pyrolysis. It was shown that hazelnut shells could be a good combustion fuel, since during its pyrolysis at high temperature, more gaseous products compared to other systems are very favored. For hazelnut shell pyrolysis, the CO_2 can be used on the large scale for the production of CO-rich syngas.

Keywords Pyrolysis of agricultural residues · Volatilization · Syngas production · H_2-rich fuel gas

Introduction

Biomass is a carbon dioxide neutral option for energy generation, and potential for conversion of biomass into energy is rapidly increasing [1, 2]. According to Maniatis [3], the energy from biomass based on short rotation forestry and other energy crops can contribute significantly toward the objectives of the Kyoto Agreement in reducing the greenhouse gas emissions and to problems related to climate change. Nevertheless, a number of biomass technologies are available for converting the biomass to energy. These processes can change raw biomass into a variety of gaseous, liquid, or solid materials that can then be used for energy generation. This conversion can be implemented in three ways: thermochemical (breakdown biomass under high temperature), biochemical (breakdown biomass under microorganism or enzymatic processes) and chemical (oils from biomass can be chemically converted into liquid fuel) [4, 5].

In recent years, there have been many developments in science and technology related to thermochemical biomass conversions so that incineration, gasification and pyrolysis conversion are among established and best available thermochemical technologies [3]. Pyrolysis processes are conducted under an inert atmosphere for the production of solids (bio-char), liquids (bio-oils), or the high heating value gases. Their relative fractions depend on the operating conditions (the extreme situations are usually referred to as slow pyrolysis [∼ 400 °C and using the slow heating rates characterized by high vapor residence time (5–30 min)] and fast pyrolysis [which mainly maximize the production of bio-oil, where the biomass is quickly heated to a high temperature with use of a very high heating rates: 1000–10.000 °C s^{-1})].

Bio-char represents the obtained solid product from pyrolysis. High values of carbon content and heating value in bio-char made it comparable to coal and coke used in blast furnaces [6]. Process parameters in pyrolysis such as temperature, heating rate, residence time, pressure, and particle size are crucial in particular to achieve a high quality of bio-char. Among the parameters, the temperature

✉ Nebojša Manić
  nmanic@mas.bg.ac.rs

1 Department of Physical Chemistry, University of Belgrade, Institute of Nuclear Sciences "Vinča", Mike Petrovića Alasa 12-14, P.O. Box 522, 11001 Belgrade, Serbia

2 Fuel and Combustion Laboratory, University of Belgrade, Faculty of Mechanical Engineering, Kraljice Marije 16, P.O. Box 35, 11120 Belgrade, Serbia

is the most influenced parameter on bio-char quality and yield. An increase in pyrolysis temperature leads to production of a better quality of bio-char, i.e., higher carbon content, lower volatiles, lower ash content, and higher heating value, whereas bio-char yield is lower when pyrolysis temperature is high, which corresponds to the poor economic performance of pyrolysis processes [7].

Through pyrolysis process, it is possible to obtain a liquid fuel with higher value-added, i.e., bio-oil. This fuel is manageable in combustion processes [8] and generates lower toxic emissions compared to those of petroleum fuels. Bio-oil is a bio-fuel obtained by condensation of vapors coming from biomass pyrolysis. However, bio-fuel is the liquid product of the fast pyrolysis of biomass.

One of the important products of the pyrolysis is a production of gas fuels (hydrogen and syngas) [9], where other valuable gases, such as carbon monoxide (CO), can also be generated by pyrolysis. These gases can be useful, among other applications, in chemical synthesis and high-efficiency combustion systems such as fuel cells. Hydrogen has been considered the most suitable alternative for future energy, aiming to reduce the dependence on fossil fuels and carbon-based emissions. The largest consumption of hydrogen includes the synthesis of ammonia and methanol, upgrading the heavy hydrocarbons and (iron) ore reduction. In addition, CO_2 reforming of methane can produce syngas with a theoretical H_2/CO ratio of one, which is lower than the H_2/CO ratio delivered by partial oxidation, steam reforming, or autothermal reforming of methane [10]. Such a syngas with a rich CO content offers the possibility to produce the syngas stoichiometries suitable for the processes of the direct synthesis of aldehydes and alcohols or olefin/gasoline synthesis of Fischer–Tropsch synthesis [11].

The main goal of this work is the characterization of gaseous products during the pyrolysis process of various agricultural residues using thermogravimetry (TG)/derivative thermogravimetry (DTG)–differential scanning calorimetry (DSC) coupled with mass spectrometry (MS) detection analysis. Since that renewable energy encompasses a very large field including wind energy and photovoltaic power, biomass is an important possibility for generating energy, and consequently, the thermal analysis is very important for the characterization of biomass for further suitable processing. Biomass can be effectively characterized by the TG–DSC–MS system. The results yield information about the composition (moisture, ash, carbon) of the biomass and the type of gases that are produced during the pyrolysis. This information allows the potential of particular biomass material as an energy source to be estimated, as well as doing beneficial to modeling and scaling-up of selected biomasses.

Materials and methods

Used materials and sampling procedure

For simultaneous thermal analysis (STA), different agricultural residue samples were used as follows: corn (*Zea mays*) brakes, wheat straw (*T. aestivum*) and hazelnut (*Corylus avellana*) shells.

Corn was grown on domestic fields in a central region of the Republic of Serbia. After peeling, corn brakes were left on a pile as industry leftovers for 2 months. Hazelnut shells came from suburban region of Serbia, near Capital city, Belgrade. After removing hazelnuts' inner part, shells were collected in bags and left for 8 months before they were brought to the laboratory. Wheat straw was brought from mountains in Southern Serbia, and it was already dried before sample preparation started.

According to standard EN ISO 14780 [12] for solid biomass fuel sample preparation, each biomass sample was prepared for experimental tests. Sample was removed from the transportation packing, and then it is placed inside the oven at 105 °C for 2 h, in order to define moisture left on the inner surfaces of the packing. This amount of moisture was included in the calculation of the total moisture content in the sample according to standard EN ISO 18134 [13]. Further, regarding to pre-drying process of the sample, which is necessary to remove the residual moisture during preparation, sample was placed on a plate and left to reach moisture equilibrium with laboratory atmosphere conditions for 24 h. After that period of time, sample was reduced in two steps using cutting mill, after which it was sieved through the 1 mm (18 mesh sizes) sieve.

Finally, the obtained undersize was declared as a general analysis sample and divided into three test portions for further testing. First portion of prepared sample was used for determination of ultimate analysis (carbon, hydrogen and nitrogen content), according to standard EN ISO 16948 [14]. The results of proximate analysis (total moisture, ash, volatile matter and char content) were obtained from the second portion of the prepared sample, according to standard procedures EN ISO 17225-1 [15]. The higher heating value (HHV) and lower heating value (LHV) for tested samples were determined using calorimeter laboratory equipment with an oxygen bomb (IKA C200, IKA® Works, Inc., Wilmington, USA), according to the standard EN ISO 18125 [16].

Simultaneous thermal analysis (STA) measurements

The STA [TG–(DTG)–DSC] measurements were performed on the third portion of the prepared biomass

sample, and all of the obtained results were used for studying the pyrolysis process.

NETZSCH STA 445 F5 Jupiter system (Erich NETZSCH GmbH & Co. Holding KG, Germany) was used for STA experimental tests for all examined samples. Inert atmosphere was provided to maintain the pyrolysis process using high purity nitrogen (Class 4.6) as a carrier gas. At the same time, nitrogen was used as a protective gas in order to keep the high sensitive internal balance (0.1 μg). Both carrier and protective gas flows were set to $\varphi = 50$ mL min^{-1}. The mass measurements were carried out using internal balance which provided the following results: corn brakes, 5.45 ± 0.10 mg, hazelnut shell, 5.35 ± 0.10 mg, and wheat straw, 5.80 ± 0.50 mg, respectively. Crucibles that were used for tests are made of alumina, and during each measurement, they were filled approximately up to the half. Crucible's lid was placed on the top, so the optimum heat transfer could be realized. Each sample was tested using three different heating rates ($\beta = 5$, 10 and 20 °C min^{-1}). Using these heating rates, the samples were heated from the room (ambient) temperature up to $T = 600$ °C. During all the measurements, the sample temperature controller (STC) was turned off, so the set temperature (600 °C) is referred to the furnace temperature. Temperatures presented on diagrams are the sample temperatures that, due to the construction of the furnace, never reached the set temperature. This fact resulted in better temperature curve linearity than it would be if STC was turned on. STA 445 F5 Jupiter runs under the versatile Proteus® software and includes all operating tools to obtain a reliable measurement and evaluate the resulting data, or even carry out complicated analyses. Obtained results from these measurements were exported and prepared for kinetic analysis.

In order to measure performance of the volatile matters release during pyrolysis, devolatilization index (D_i) [17] was defined:

$$D_i = \frac{(-R_{\max}) \cdot (-R_{\mathrm{avg}})}{(T_{\mathrm{in}} \cdot T_{\max} \cdot \Delta T_{1/2})}, \tag{1}$$

where $R_{\max}$ is the maximum mass loss rate, R_{avg} is the average mass loss rate, T_{in} is the initial devolatilization temperature of the process, $T_{\max}$ is the temperature when mass loss rate reaches maximum value, and $\Delta T_{1/2}$ is the temperature interval when instantaneous mass loss rate (R_d—is the decomposition rate) equals to the half of $R_{\max}$.

Mass spectrometry (MS) analysis

Determination of evolved gases from performed STA was carried out continuously, using quadrupole mass spectrometer NETZSCH QMS 403 D Aëolos (QMS) (Erich

NETZSCH GmbH & Co. Holding KG, Germany). TGA/STA–QMS coupling was done using transfer line with quartz capillary tube with diameter of 75 μm. The whole transfer line was heated up to 230 °C in order to avoid condensation of evolving volatile compounds. The QMS was operated under vacuum up to 10^{-7} bar, providing conditions necessary to detect gas components using their ions intensity according to their respective mass to charge ratios (m/z). Evolved gas composition was monitored and analyzed through bar-graph cycles, scanning mass units in the range from 1 to 80. Cycles were set to speed of 0.2 s per mass unit and carried out using stair mode. The excitation energy in the QMS was set up at 1200 eV with the resolution of 50 units.

From the selected range, the focus was on the specific ions that correspond to gases evolved in the pyrolysis process. Accordingly, the molecules with atomic mass units (amu) of 2, 16, 18, 28, 30, 44, 58 and 72 which correspond to H_2, CH_4, H_2O, CO, C_2H_6, C_3H_8 (CO_2), C_4H_{10} and C_5H_{12}, respectively, were analyzed, and the intensity peak areas obtained for each compound were compared.

Results and discussion

Results of proximate and ultimate analysis and bio-char yields

Table 1 shows the results of proximate and ultimate analysis of various agricultural residues.

It can be seen from Table 1 that all samples are characterized by high volatile matter, ranging from 65.32 to 73.94%, which makes them desirable for a good regulation of combustion or gasification processes. Among tested samples, wheat straw shows the highest ash content value (7.88%), because of the fact that among all agricultural residues, high ash contents of straws [18] interfere with pulping process (apropos water must be spray onto the wheat straw when cutting it in pulp mill to prevent raising of dust), the chemical recovery of pulping chemicals, and the utilization of straws as fuels. Raw materials have moisture content in a range 8.58–11.63%, which can be attributed to open air conditions. From a theoretical point of view, corn brakes can be suitable for good production of bio-oil, while hazelnut shell would be the best agricultural residue for production of bio-char. All tested samples have HHV values ranging from 15.29 to 18.20 MJ kg^{-1}, which belongs to heating values of biomass derived bio-chars (11.83–44.20 MJ kg^{-1}) [19, 20]. Generally, samples with high HHV values make them very attractive for the source-feeds for clean energy production instead of fossil-based solid fuels (hazelnut shells stand out).

Table 1 Proximate and ultimate analysis results for various agricultural residues

Proximate analysis/mass%		Ultimate analysis[b]/mass%	
Corn brakes			
Moisture	8.58	C	47.97
Volatile matter	73.94	H	6.87
Fixed carbon	16.00	O[c]	42.89
Ash	1.48	N	0.66
HHV/MJ kg^{-1}	16.72	S	0.00
LHV[a]/MJ kg^{-1}	15.10		
Proximate analysis/mass%		Ultimate analysis[b]/mass%	
Wheat straw			
Moisture	11.63	C	44.12
Volatile matter	65.32	H	6.34
Fixed carbon	15.17	O[c]	39.99
Ash	7.88	N	0.63
HHV/MJ kg^{-1}	15.29	S	0.00
LHV[a]/MJ kg^{-1}	13.91		
Proximate analysis/mass%		Ultimate analysis[b]/mass%	
Hazelnut shell			
Moisture	9.27	C	50.12
Volatile matter	68.08	H	6.66
Fixed carbon	20.97	O[c]	40.53
Ash	1.67	N	0.86
HHV/MJ kg^{-1}	18.20	S	0.00
LHV[a]/MJ kg^{-1}	16.68		

[a] Calculated according to EN ISO 18125

[b] On a dry basis

[c] By the difference

In addition, the concentration of C and H is lowest for wheat straw, while their highest concentration was identified for hazelnut shell (Table 1). Wheat straw has a something lower content of O compared to other samples, which may indicates on the creation of smaller amounts of inorganic vapors in combustion processing. However, all samples show the presence of oxygen more than 30% which means that they can be essential in deoxygenation. Agricultural biomass has a low heating value due to its high ash content [21], where it was reported [22] that biomass with a high ash content is not an ideal fuel source, because the ash content is one of the main factors that directly influence the heating value of biomass. High carbon and low oxygen in biomass as compared to the coal are favorable for combustion applications, while higher proportion of carbon (relative to hydrogen and oxygen content) (for wheat straw and hazelnut shells, Table 1)

increases energy content of a fuel because the energy contained in carbon–carbon bonds is greater than that of carbon–oxygen and carbon–hydrogen bonds [23].

TGA–DTG–DSC curves of pyrolysis process of various agricultural residue samples

Figures 1–3 show experimental TG (thermogravimetric)–DTG (derivative thermogravimetric)–DSC (differential scanning calorimetry) curves for thermal decomposition of corn brakes (a), wheat straw (b) and hazelnut shell (c), under an atmosphere of nitrogen.

Considering TG curves (Fig. 1), it can be observed that with an increase in heating rate, the TG curves are shifted to the right, i.e., that the mass losses occur at increasing temperatures. This behavior has been described by several researchers and can be explained using different arguments [24, 25]. Some authors argue that this behavior is due to changes in reaction mechanism caused by increased heating rate. Furthermore, poor heat transmission to the sample in the oven may cause increasing differences with increasing heating rate between the nominal and real temperature of the sample. It could also be due to different rates of heat dissipation or absorption of the reaction at the different heating rate. However, the observed shift can be explained by mathematical form of kinetic laws, which can provide a shift of the curves at higher temperatures with increasing reaction rate with possible same kinetic constants.

All TG curves (Fig. 1) show three main stages which are typical for biomass pyrolysis. The first stage corresponds to moisture release (water evaporation) (pre-pyrolysis stage), which is approximately performed in the temperature range 25–175 °C. The remaining two stages are attributed to active and passive pyrolysis, respectively. The active pyrolysis stage is characterized by largest mass loss where various vapors and gases are released as a result of decomposition processes of hemicelluloses and cellulose which takes place in this stage, within temperature ranges 175–380 °C and 250–380 °C [26], respectively. A variety of volatiles would have been released during this stage, resulting in a drastic mass loss, decomposition of cellulose and hemicelluloses, along with the formation of the major pyrolytic products. On the other hand, the lignin is decomposed in both stages: active and passive pyrolysis stages in the temperature range 175–600 °C, without characteristic peaks (Fig. 2). Furthermore, lignin mainly contributed toward bio-char production as a higher content of lignin in biomass, resulting in higher bio-char production and the higher thermal stability.

However, the various agricultural residues show different heat effects with respect to the number of endothermic and exothermic peaks at fixed heating rate (Fig. 3). The
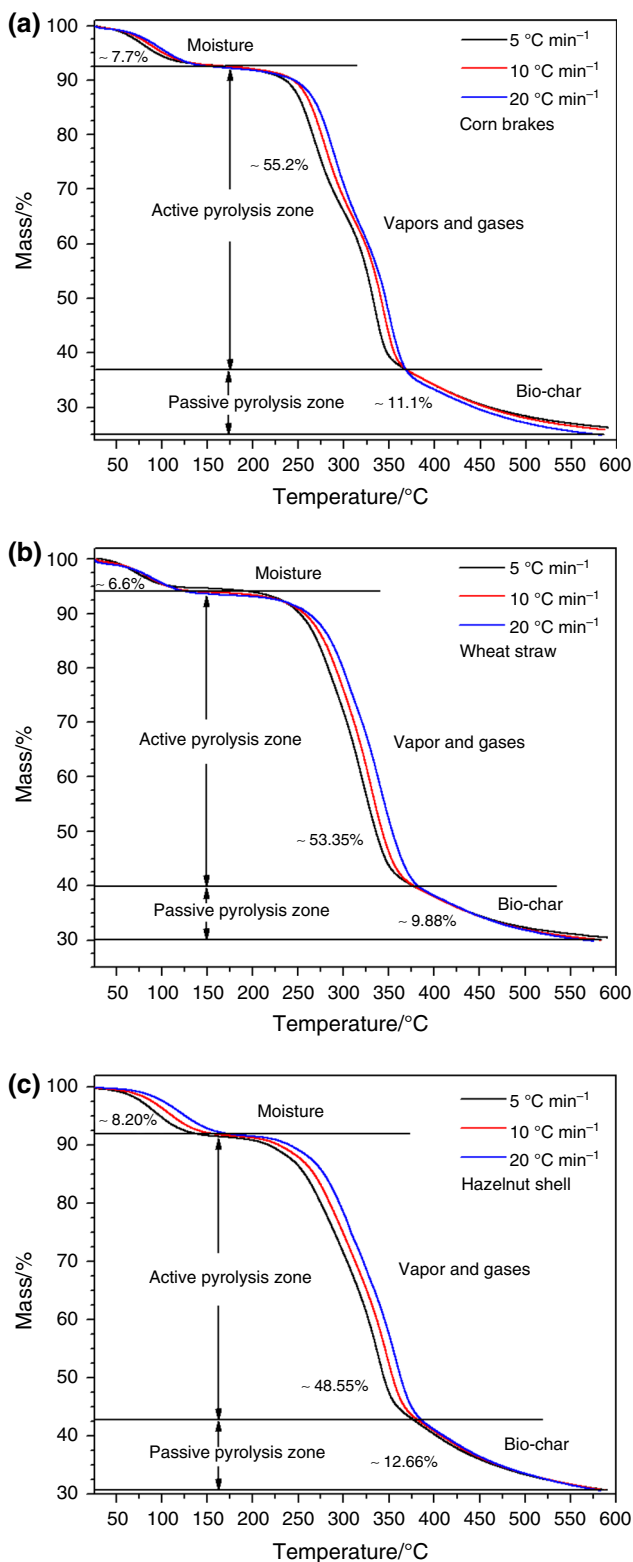
Fig. 1 TGA curves of **a** corn brakes, **b** wheat straw, **c** hazelnut shell at the different heating rates (5, 10 and 20 °C min^{-1})

depth of endothermic peak related to pre-pyrolysis stage varies from sample to sample, which is in correlation with moisture content in the samples (Table 1). The two
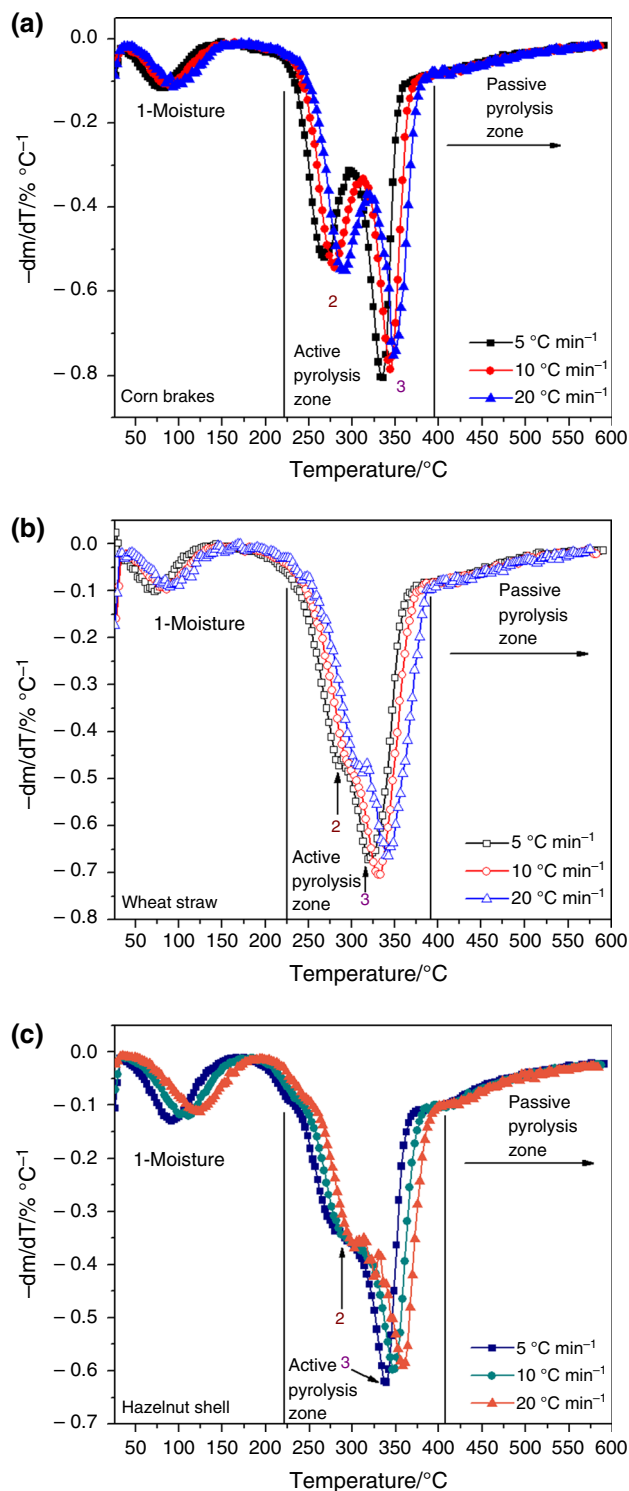
Fig. 2 DTG curves of **a** corn brakes, **b** wheat straw, **c** hazelnut shell at the different heating rates (5, 10 and 20 °C min^{-1})

endothermic peaks at the DSC curves that can be attributed to decompositions of hemicelluloses and cellulose in active pyrolysis do not appear in all samples, and this is especially refers to wheat straw (Fig. 3). One of the processes is certainly "masked" given that probably there is an

advantage of overlapping decomposition reactions, related to one of the pseudo-components in the samples. The DSC curve for hazelnut shell is only distinguished from other DSC curves. Certain variations in the heat effects can be
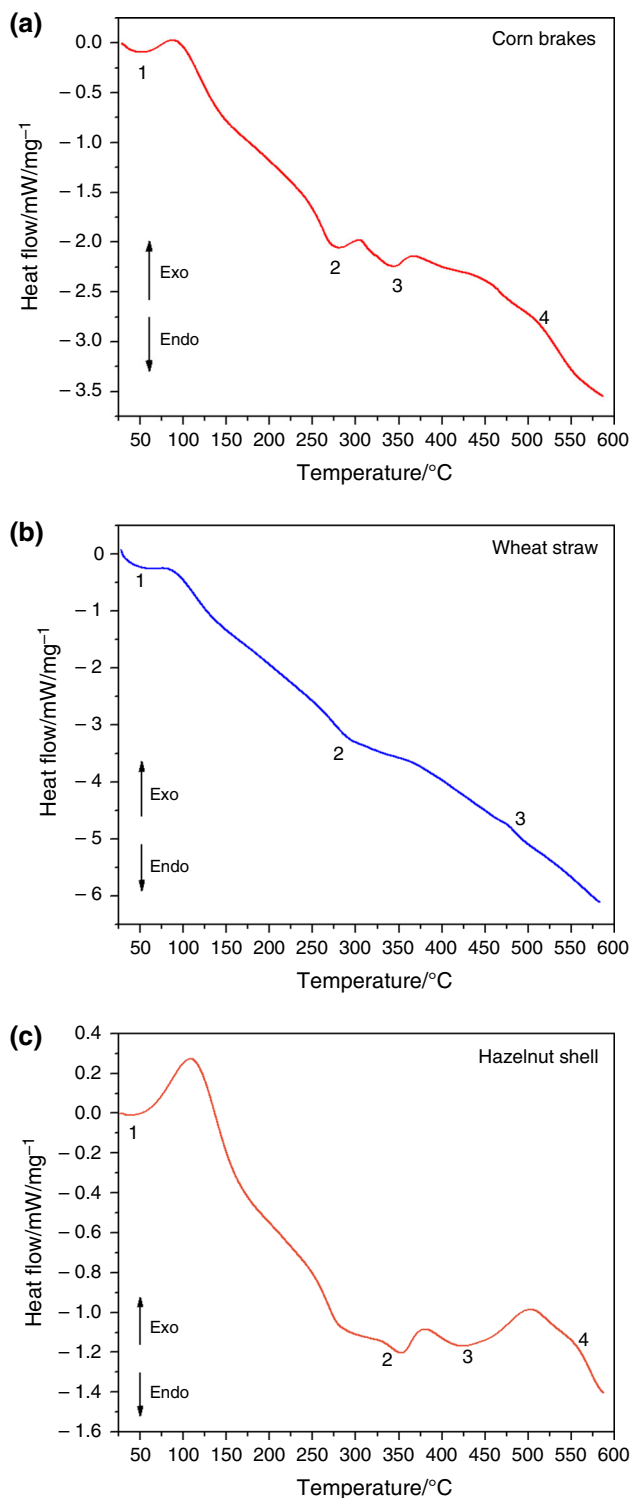
significantly stimulated by concentration of the three pseudo-components (hemicelluloses, cellulose, and lignin) present in samples, which also affects development of decomposition paths. This means that the observed reaction probably follows different mechanism owing to the changing composition of the residual biomass. For wheat straw, the slight exothermic effect in passive pyrolysis which is attributed to bio-char forming was designated by "3," while for other samples this is indicated by "4" (Fig. 3).

Regardless of the pyrolytic behavior, only the DTG curve related to corn brakes (Fig. 2a) shows two distinctive peaks attributed to hemicelluloses and cellulose decomposition reactions in an active pyrolysis stage. For other two agricultural residues (wheat straw and hazelnut shells) (Fig. 2b, c), the well-defined peak which was present in corn brakes pyrolysis is transformed into the "shoulder." Considering all DTG curves (Fig. 2), the long tails in a passive pyrolysis stage can be attributed to decomposition of lignin at the temperatures above 400 °C, where pyrolysis proceeds with a slower mass loss rate.

Based on these results, it can be concluded that at the high heating rates, separate DTG peaks did not arise because some of them were decomposed simultaneously and several adjacent peaks were united to form overlapped boarder and higher peaks. This is consequence of heat and mass transfer limitations. In this respect, with an increase in the heating rate, the temperature in furnace space can be a little higher as the temperature of a particle and the rate of decomposition are higher than the release of volatiles. Differences in molecular structures and chemical nature of three pseudo-components account for dissimilar observed behaviors. Namely, it is obvious that variations in appearance in the DTG curves are primary related to variation in percentage of hemicelluloses presented in biomass samples. Namely, the higher lignin content may lead to a slower decomposition with a more energy needed, whereas higher cellulose and hemicelluloses content decomposes faster and produces a larger fraction of gaseous products.

Detected exothermic effects within passive pyrolysis stage can be attributed to decomposition patterns of hemicelluloses and lignin that are related to their high charring nature, and which is in contrast with the decomposition of cellulose taking place by the full volatilization [27]. Bio-char consists of the residue of lignin [28], where lignin continues to further exothermic polymerization stage of bio-char. At higher temperatures, polymerization of biomass bio-char continuously occurred and polymerization reaction is dependent on unique properties of bio-char of the sample.

Fig. 3 DSC curves of **a** corn brakes, **b** wheat straw, **c** hazelnut shell recorded at $\beta = 10$ °C min^{-1}

Devolatilization analysis

Table 2 lists characteristic parameters of initial temperature (T_{in}), the maximum (peak) temperature (T_{max}) of the main mass losses, along with the maximum decomposition rate (R_{max}), the temperature interval when R_d/R_{max} equals ½ ($\Delta T_{1/2}$), and the volatile release index (D_i) at the various heating rates (5, 10, and 20 °C min^{-1}).

It can be seen from Table 2 that all values increase with increased heating rate. The maximum decomposition rate tended to rise at relatively faster heating rates [29, 30]. This effect was attributed to the fact that more thermal energy is released at the faster heating rates, which promotes thermal transmission nearby and within sample. For all samples, the volatile release index reaches its highest value at the highest heating rate.

Corn brakes started to decompose at lower temperature, while other samples are characterized by very similar T_{in} values. Similar T_{in} values were primarily governed by content ratio of hemicelluloses, cellulose, and lignin, so that similar values can also be expected for kinetic decomposition parameters. Namely, the polymers of hemicelluloses, cellulose and lignin were mainly linked with the ether bonds, which exhibited relatively lower bond energy and can crack at the lower temperatures, which, for

example, is the opposite in the case of coal (consists of the dense polycyclic aromatic hydrocarbons, connected by C=C aromatic bonds) [31]. It can be concluded that with an increase in heating rate, D_i shows an upward trend, and the more easily the volatiles were released.

## Analysis of the gases produced during pyrolysis

Thermogravimetry–mass spectrometry (TG–MS) profiles of evolved gases during pyrolysis, H_2, CH_4, C_2H_6, C_4H_{10}, C_5H_{12} and profiles of the changes in the ion current as a function of temperature (the mass spectra) for pyrolytic water (H_2O), CO_2 (C_3H_8) and CO for agricultural residues (CB—corn brakes, WS—wheat straw, and HS—hazelnut shell) at the different heating rates of $\beta = 5$, 10 and 20 °C min^{-1} are shown in Figs. 4–6a–i.

The present study was focused on the main volatile products of biomass pyrolysis on the basis of changes in ion currents across the temperature range of 40–600 °C, and on their relevancy, assigned to the ion/mass intensities (m/z) with corresponded screening analysis performed in the selected-ion monitoring (SIM) mode (the ions characteristic of each molecules: 2, 16, 18, 28, 44, … for H_2, CH_4, H_2O, CO, CO_2, … were monitored) which is in

Table 2 Pyrolysis feature parameters of various agricultural residues under the different heating rates ($\beta = 5$, 10 and 20 °C min^{-1})

Sample at 5 °C min^{-1}	Corn brakes		Wheat straw	Hazelnut shell
Parameters	(2)[a]	(3)[a]	(3)[a]	(3)[a]
R_{max}/% min^{-1}	− 2.72434	− 4.15587	− 3.45351	− 3.17349
T_{in}/°C	248.90	321.95	252.62	250.76
T_{max}/°C	267.65	332.78	321.78	336.63
$\Delta T_{1/2}$/°C	31.81	22.35	78.79	56.16
D_i/%^{2} °C^{-3} min^{-2}	8.62 × 10^{-7}	1.16 × 10^{-6}	3.40 × 10^{-7}	4.20 × 10^{-7}
Sample at 10 °C min^{-1}	Corn brakes		Wheat straw	Hazelnut shell
Parameters	(2)[a]	(3)[a]	(3)[a]	(3)[a]
R_{max}/% min^{-1}	− 5.87940	− 8.33932	− 7.40228	− 6.28740
T_{in}/°C	256.34	333.13	267.52	263.80
T_{max}/°C	279.03	343.96	330.61	346.46
$\Delta T_{1/2}$/°C	30.08	22.49	71.20	76.78
D_i/%^{2} °C^{-3} min^{-2}	3.82 × 10^{-6}	4.52 × 10^{-6}	1.54 × 10^{-6}	1.17 × 10^{-6}
Sample at 20 °C min^{-1}	Corn brakes		Wheat straw	Hazelnut shell
Parameters	(2)[a]	(3)[a]	(3)[a]	(3)[a]
R_{max}/% min^{-1}	− 12.61400	− 16.68326	− 14.60554	− 12.99792
T_{in}/°C	263.80	335.00	271.25	278.84
T_{max}/°C	291.72	347.75	342.41	358.25
$\Delta T_{1/2}$/°C	28.07	18.77	82.51	82.52
D_i/%^{2} °C^{-3} min^{-2}	1.74 × 10^{-5}	2.28 × 10^{-5}	5.30 × 10^{-6}	4.37 × 10^{-6}

[a]Related to corresponding DTG peaks in Fig. 2
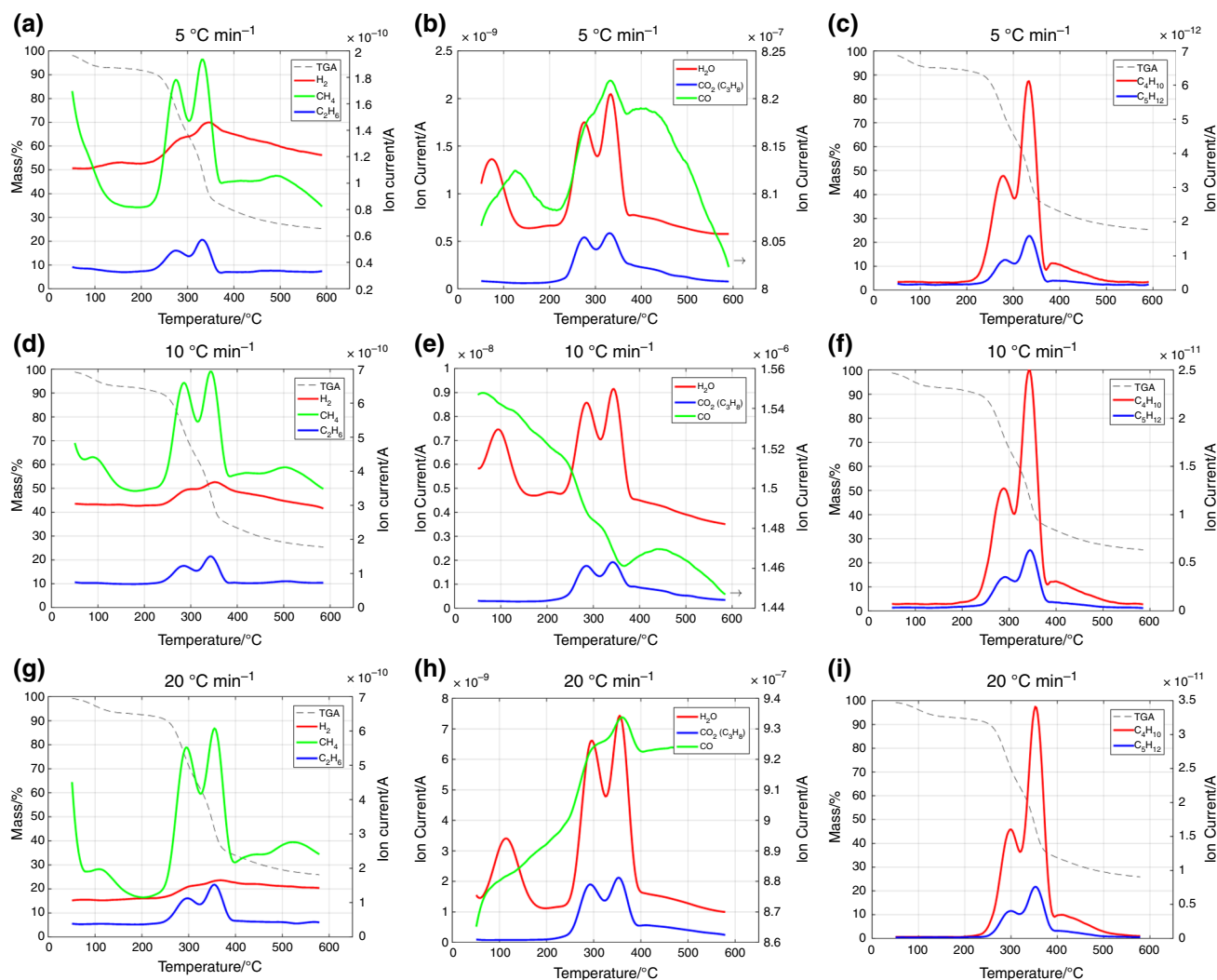
Fig. 4 Simultaneous TGA–MS profiles of evolved gases during pyrolysis of corn brakes (CB)

accordance with database of National Institute of Standards and Technology (NIST).

For all samples, the primary devolatilization stage was identified with major mass loss and the release of organic compounds which leads to formation of bio-char, where this stage releases H_2, CH_4, H_2O, CO_2 (also C_3H_8), CO, including the light hydrocarbons (Figs. 4–6). The maximums in DTG curves (Fig. 2) correspond to the maximum gas releases, as shown in Figs. 4–6. It can be observed that with an increase in the heating rate, the "intensity" of the ion current also increases, so that the rate of release of the gas products is higher. For CB and WS, the light gases, H_2, CH_4 (C_2–C_5), and CO_2 evolve at a wide temperature range and their evolution profiles are similar to DTG maximum rates. In addition, some deviations are observed for CO evolution profile and this profile varies with changing of the heating rate. The largest deviation shows the CO evolution profile for HS pyrolysis with respect to DTG

maxima features, and this deviation is particularly pronounced, when changing the heating rate from lowest to highest rate of heating. This is consequence of non-profiled DTG peak, with clear appearance of "shoulder," which in many cases depends on hemicelluloses concentration (if concentration is quite low).

Having in mind these results and comparing CO gas profiles (including CO_2 profile) for all agricultural residues, it can be concluded that contribution of lignin also plays a significant role and its contribution largely depends on the rate of heating. Since lignin is decomposed continuously in a wide temperature range, with undefined rate of the mass loss, such behavior is manifested through a series of "unsteady" profiles of CO evolution.

It should be noted that for all cases observed, the CH_4 and H_2 peaks are detected in passive pyrolysis zone for $T > 450$ °C. Such secondary pyrolysis is the result of decomposition of heavy molecules in bio-char. The H_2
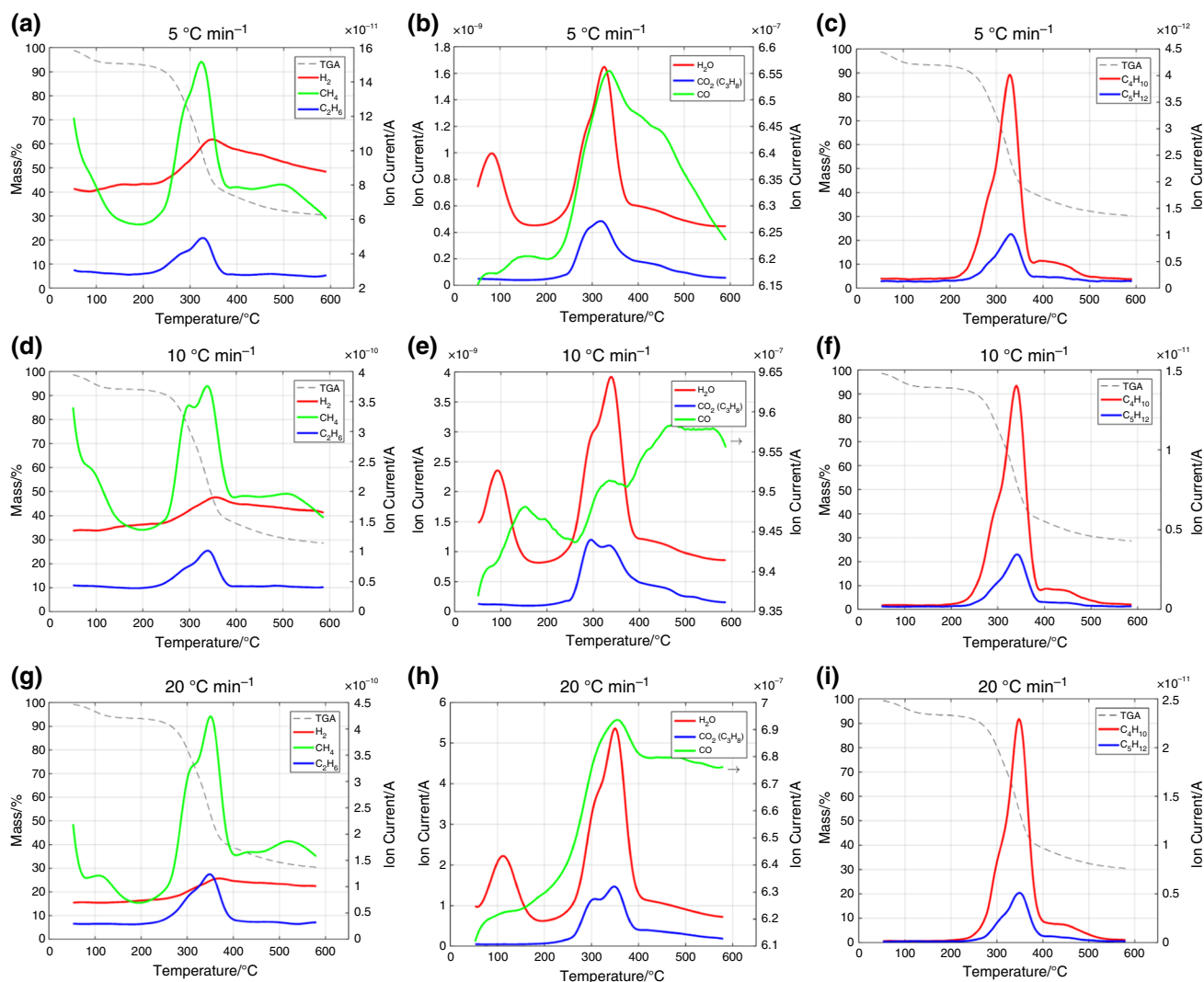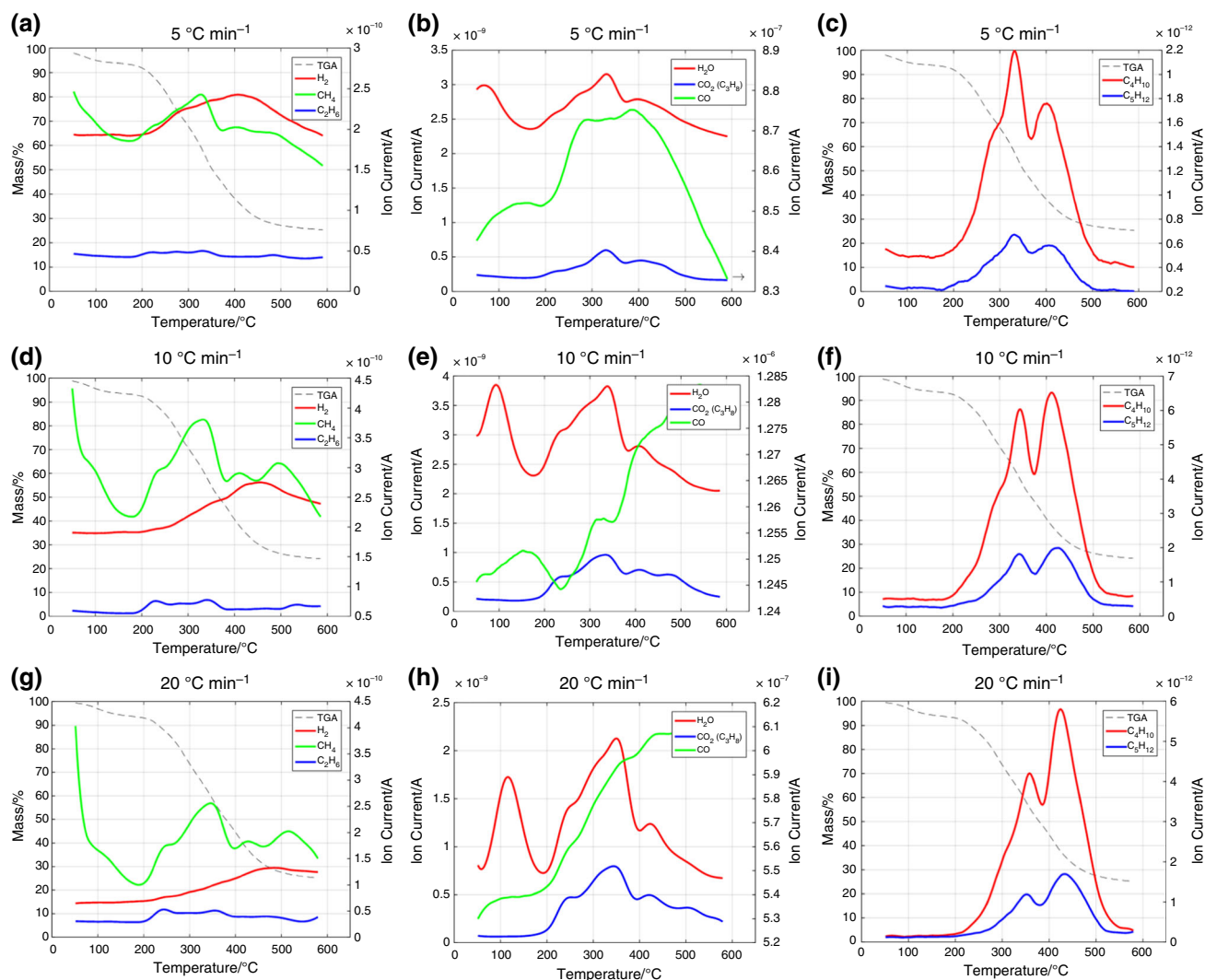
Fig. 5 Simultaneous TGA–MS profiles of evolved gases during pyrolysis of wheat straw (WS)

evolved is, in fact, only a part of hydrogen present due to higher volatile matter content in the samples. Hence, observed decomposition is a complex process which involves devolatilization and pyrolysis, essentially based on chemical constituents of the samples.

It should also be noted that for HS, two local maxima at 10 and 20 °C min^{-1} in the temperature ranges 400–450 °C/450–550 °C (Fig. 6a, d, g) correspond to methane evolution peaks. The lower temperature peak can be attributed to –OCH$_3$ functional group cracking, while higher temperature peak is due to charring processes [32].

A relatively significant amount of CO and H$_2$O are detected because of large number of hydroxyl groups and oxygen atoms present in samples (cellulose, hemicelluloses, and lignin). However, we can note that majority of gases is generated in temperature range of 200–500 °C, where differences occur with respect to change in the heating rate.

At temperatures below 200 °C, there is just the production of H$_2$O; its peaks coincide with those of DTG curves, during evaporation step. The release of H$_2$O and CO$_2$ (C$_3$) takes place between 200 and 500 °C. These two gases are characterized mainly by two peaks, where H$_2$O was produced on all the interval of decomposition of the samples, what indicates on their provenance from different origins. The peak obtained at approximately at 105 °C is due to the liberation of absorbed water, while the peaks beyond 200 °C correspond to the water formed during the decomposition of hemicelluloses, cellulose and lignin [32, 33]. The productions of C$_2$H$_6$ result from decomposition of cellulose, while the release of CH$_4$ at low temperatures comes from decompositions of cellulose and hemicelluloses [34]. At high temperatures, CH$_4$ is mainly produced by the cracking of the methoxyl groups [35].

Fig. 6 Simultaneous TGA–MS profiles of evolved gases during pyrolysis of hazelnut shell (HS)

Figure 7a–h shows simultaneous comparison of individual gaseous products for each sample at a fixed value of the heating rate ($\beta = 10$ °C min^{-1}).

Shape similarities of the mass spectra of these compounds with shapes of DTG curves for all samples are obvious. On the other hand, however, the hydrogen signal has a different behavior. At a fixed rate of the heating, for WS, the ion current of hydrogen increases from low temperature to approximately 350 °C and then decreases to higher temperatures (Fig. 7a). However, for CB, the ion current of hydrogen increases also from low temperature and maintains at a constant value in a very narrow temperature range and then increases up to 340 °C and then decreases to higher temperatures (Fig. 7a). Considering DTG curve for actual system at 10 °C min^{-1}, it can be observed that there are some differences with behavior of the mass signal. The largest differences can be seen in the case of HS, where the maximum ion current is reached at

approximately 460 °C, which is completely opposite to the maximum mass loss rate identified on DTG curves (Fig. 2). In this case, it can be assumed that the mass spectrometric signal is strongly overlapping with DTG peak. For CB, the mass spectrometric signal for hydrogen is overlapping only partially with DTG curve. From these results, it can be concluded that the main source for hydrogen production arises from thermal volatilization of biomass pseudo-components [36]. The methane mass spectrometric signal for all systems (except for HS) is similar to the shape of DTG curves. However, for CB and HS, the methane signals show the broad peaks in the temperature ranges 450–580 °C and 460–580 °C, respectively.

This means that in considered cases, the most pronounced sources for methane production come from two origins: volatilization at lower temperatures and charring process at high temperature. For volatilization, the cleavage of methoxyl groups present in lignin is more important
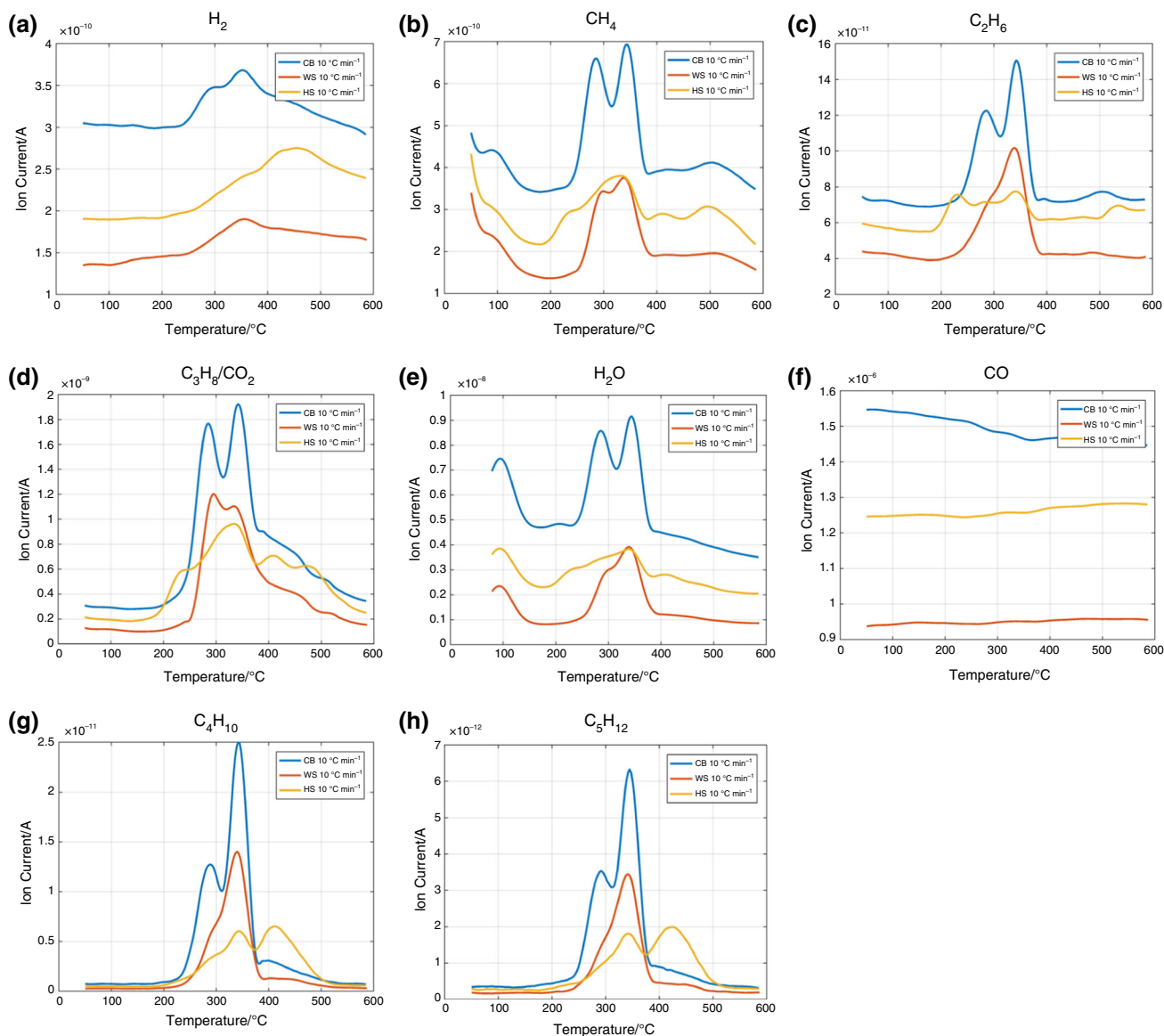
Fig. 7 Comparison of individual gaseous products for CB, WS and HS at a fixed heating rate ($\beta = 10$ °C min^{-1})

here. At high temperatures, the CH_4 production is attributed to charring processes which involve aliphatic and aromatic chars. The broad peaks in the high temperature zone can be explained on the basis on the fact that methane could be obtained from bio-char in the current temperature ranges.

At the lower temperatures, the mass signals of H_2O, CO and CO_2 evolutions are due to volatilization of hemicelluloses and partially of cellulose (CO was most likely generated from cellulose pyrolysis) [36]. Distinct emission of CO_2 appeared from 200 °C, and it reached a high mass spectrometric peak within 300–400 °C, which is the major pyrolysis zone of celluloses. The peak around 350 °C was ascribed to decomposition of aromatic and aliphatic carboxyl groups in celluloses. It can be assumed that below 500 °C, the abundant presence of C=O groups in hemicelluloses can be favorable for CO_2 emission. As temperature increased, the more stable ether structures and oxygen-bearing heterocycles in lignin are also decomposed into the CO_2.

Consistent with the distribution of mass signals related to H_2O, CO and CO_2 evolutions for all samples, we can assume that most important volatiles source is the lignin, followed by the cellulose, and finally hemicelluloses [35, 36]. Compared to hemicelluloses and lignin, cellulose released most of gaseous products in a narrow temperature range (300–400 °C). On the other hand, the hemicelluloses and lignin released methane and –CH_3 groups at about 500 °C. Consequently, the methane was generated at about 420 °C from hemicelluloses and at about 500 °C from

lignin. However, the highest concentration emission of methane occur about 380 °C. The methane emission at relatively lower temperatures was probably released from C–C bond cleavage in aliphatic chains, whereas methane emission at higher temperatures was mainly produced from cracking of a weakly bonded methoxyl-O–CH_3 group as well as break of having higher bond energy of methylene group –CH_2 [37]. Considering biomass pseudo-components pyrolysis, the methane was mainly released from pyrolysis of lignin, because it contains more methoxyl–O–CH_3 chemical groups than the hemicelluloses and celluloses.

In addition to above considerations, hydrogen formation which arises at high temperatures (> 450 °C) can be attributed to secondary reactions as steam reforming and/or tar cracking [38, 39]. At lower temperatures, the hydrogen emission was mainly generated from thermal decomposition of cellulose and hemicelluloses. At $T > 450$ °C, the decreasing trends in hydrogen mass signal may reveal that lignin pyrolysis could also generate the hydrogen.

In order to estimate the amount of energy received from syngas realized by studied agricultural residues, the corresponding H_2/CO ratios were analyzed. Figure 8 shows dependency of H_2/CO ratios on the temperature. For all samples, the H_2/CO ratios are below 1.00 for temperatures below 350 °C. Only in the case of HS pyrolysis, the H_2/CO ratio is equal to 1.00 at about 445 °C (Fig. 8).

This behavior which is present for HS can be associated with highest value of LHV (16.68 MJ kg^{-1}; Table 1). The HS can be a good combustion fuel, since during its pyrolysis at high temperature, more gaseous products compared to other systems are very favored. In the latter case, the high temperatures favor higher CO and H_2 production. Considering syngas, which is ideal product
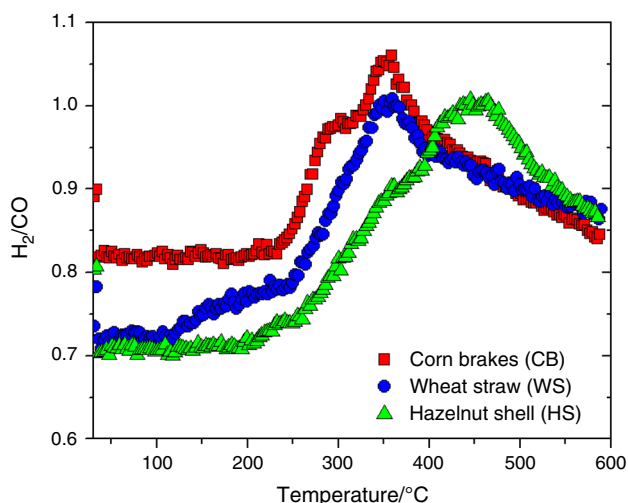
consisting of hydrogen and carbon monoxide and dioxide, the higher temperatures are ideal. This can also be seen on the basis of the mass spectrometric signal for hydrogen at fixed rate of heating, where high hydrogen contribution was observed at high temperatures. So, for HS, the CO_2 can be used on the large scale for production of CO-rich syngas with a H_2/CO ratio equal to the unity, at fixed temperature of 445 °C. On the other hand, for CB, the H_2/CO ratio which amounts 1.06 at 358 °C is convenient for reforming of methane that typically achieves H_2/CO ratios above the unity. Such syngas enriched with CO contents is suitable for production processes of various chemicals [40, 41].

Table 3 shows the characteristic temperature values [such as initial (T_i), peak or maximum (T_p) and end (final) (T_{end}) temperatures] related to the release of gaseous products, with target gaseous releasing ion currents (for H_2, CH_4 and CO) as well as the maximum temperature ratios for H_2/CO, considering pyrolysis process of hazelnut shell (HS), corn brakes (CB), and wheat straw (WS) samples. The results are presented for the heating rate of $\beta = 5$ °C min^{-1}.

From the results presented in Table 3, it can be observed that for HS sample, all monitored non-condensable gases (H_2, CH_4, and CO) are released at lower initial temperatures and much earlier compared to other samples. On the other hand, the maximum and end temperatures vary from sample to sample, making them highly dependent on the type of biomass, but also on the observed heating rate (Table 3). However, considering all samples, it can be identified that both T_p and T_{end} for H_2 and CO gases are characterized by high values, where combination of low heating rate and high temperatures (allowing longer gas residence time) can affect on gas pyrolysis yields. So, the reaction temperature of pyrolysis process affects both on the composition and yield of gaseous products. It should be noted that increasing the temperature leads to increases of CO. Regarding HS, CB and WS samples pyrolysis, it can be seen that the maximum rate (relatively to ion current magnitude) of methane evolvement occurs (excluding the CO gas) earlier for WS pyrolysis, in comparison with other pyrolytic processes. This is obviously consequence of the fact that the methane is released from lignin structures but in a simpler mechanism, since the WS is poorer with lignin content (∼ 15%) [42], allowing its maximum release at a much lower T_p value, reflecting through reduced IC_p value (Table 3). Considering higher values for "peak" and "end" pyrolysis sections attached to T and IC quantities, the CO gas evolving characteristics during HS pyrolysis dominate in comparison with other studied samples. This is in accordance with the results shown in Fig. 8. Also, the observed properties presented in Table 3 are reflected through the maximum temperature ratio values for H_2/CO,

Fig. 8 Dependency of H_2/CO ratios on the temperature for the pyrolysis of various agricultural residues

Table 3 The characteristic gas evolving temperatures values [initial—T_i, peak (maximum)—T_p, and the end—T_{end}] and the corresponding ion current values attached to target signals at $\beta = 5$ °C min^{-1}, considering H_2, CH_4 and CO gases releases, during CB (corn brakes), WS (wheat straw), and HS (hazelnut shell) pyrolysis processes

HS sample	T_i/°C	IC_i/A	T_p/°C	IC_p/A	T_{end}/°C	IC_{end}/A	Maximum temperature ratio for H_2/CO
H_2	207.6	1.944×10^{-10}	405.1	2.429×10^{-10}	592.7	1.929×10^{-10}	1.08
CH_4	190.8	1.874×10^{-10}	332.4	2.422×10^{-10}	369.5	1.996×10^{-10}	
CO^a	209.1	8.527×10^{-7}	374.6	8.754×10^{-7}	593.2	8.331×10^{-7}	

CB sample	T_i/°C	IC_i/A	T_p/°C	IC_p/A	T_{end}/°C	IC_{end}/A	Maximum temperature ratio for H_2/CO
H_2	212.7	1.153×10^{-10}	345.9	1.476×10^{-10}	593.3	1.219×10^{-10}	1.02
CH_4	226.9	0.868×10^{-10}	337.0	2.068×10^{-10}	371.2	1.032×10^{-10}	
CO^a	231.5	8.095×10^{-7}	338.0	8.231×10^{-7}	593.3	8.019×10^{-7}	

WS sample	T_i/°C	IC_i/A	T_p/°C	IC_p/A	T_{end}/°C	IC_{end}/A	Maximum temperature ratio for H_2/CO
H_2	221.9	0.804×10^{-10}	346.2	1.068×10^{-10}	593.6	0.876×10^{-10}	1.05
CH_4	241.4	0.670×10^{-10}	322.7	1.572×10^{-10}	368.8	0.815×10^{-10}	
CO^a	235.6	6.232×10^{-7}	330.6	6.556×10^{-7}	413.1	6.461×10^{-7}	

^{a}MS ion current signal envelopes the N_2 and CO gases releasing, but when CO gas reaches detection limit, only CO can be identified. It was known that the CO release occurs during cracking of structures and secondary reactions, but m/z of the carrier gas (N_2) does not allow the precise detection of CO evolution

where the last discussed item was related to the highest value amounted 1.08 for HS sample.

Figure 9 shows the H_2, CH_4, and CO gas product yields for HS, CB, and WS pyrolysis processes, where results are estimated from the MS spectra characteristics such as total MS peak area and the gas spreading temperature intervals.

Among all tested samples, it can be seen that the HS shows the highest yields of H_2 and CO gaseous products (Fig. 9a), which means that HS exhibits more "bio-energy" compared to other samples, because of its high hydrogen and carbon monoxide yields. It can be noticed that the difference between gas products, mainly composed of H_2, CH_4, and CO, with respect to HS, CB, and WS, is a consequence of biomasses characteristics, particle sizes, the heating rate, temperature, the product vapor residence times, etc. Among these parameters, the effect of reaction temperature is the most critical. Namely, the gas yield increased but the liquid product yield usually decreased, with the increase in reaction temperature. This frequently imply that, when the product vapors are released by devolatilization of biomass pyrolysis, more hydrocarbons in vapors can be converted into permanent gases at the higher reaction temperatures. From established results in Fig. 9, we may see that HS sample (and so on the CB sample) is very good biomass feedstock for the production of H_2-rich fuel gas. Also, the applied experimental conditions for performing the laboratory pyrolysis dynamic tests are obviously convenient for producing more H_2 and CO but less CH_4. So, the gas product of the HS slow pyrolysis can provide more bio-energy due to its higher heating value

(Table 1). However, the high hydrogen content of the gas product could be attributable to the water gas reaction: $C + H_2O \leftrightarrow CO + H_2$, where the H_2 formation may also be attributable to the cracking and reforming reactions of hydrocarbons [43]. It should be noted that lignin plays an important role for the production of gases except the CH_4, and its effect on hydrogen production can be stronger than that of the cellulose.

The presented investigation of pyrolysis process of various agricultural residues shows potential of the use of selected types of biomass as the energy suppliers instead of fossil fuels and impacts of its fractions on the thermal decomposition process, where the HS biomass feedstock shows increased fuel energy density. Energy and environment policies affect the future of agricultural fuels. The mass that the policy makers attach to the greenhouse effect is of vital importance. Sustainable energy supply by means of balanced political steering instruments increases the demand for bio-fuels and makes it possible for agricultural fuels to expand.

Conclusions

This work presented the experimental study of pyrolysis process of various agricultural residues [corn brakes (CB), wheat straw (WS), and hazelnut shell (HS)] using simultaneous thermal analysis (STA)–mass spectrometry (MS) techniques, in an inert atmosphere.
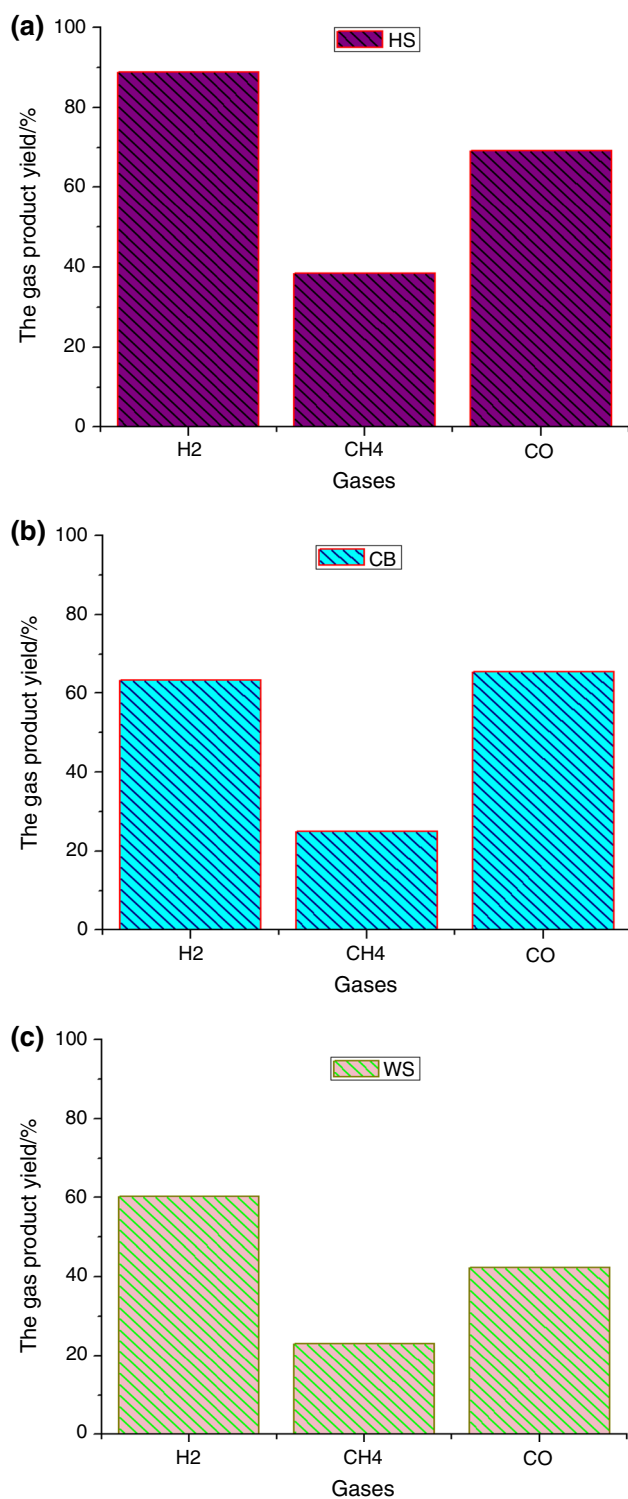
Fig. 9 The gas product yields for mainly evolved gases such as H_2, CH_4, and CO during hazelnut shell (HS) (a), corn brakes (CB) (b), wheat straw (WS) (c) slow pyrolysis processes. The gas product yield values were calculated from the total MS peak area, which includes also the gas spreading temperature intervals

The following conclusions can be drawn from this study:

1. TG and DTG results showed that the pyrolysis was represented by three successive steps: the first step corresponded to evaporation of moisture, while the second and third steps can be attributed to active and passive pyrolysis, respectively. The active pyrolysis stage is characterized by the largest mass loss where various vapors and gases are released as a result of decomposition processes of hemicelluloses and cellulose. The third pseudo-component of biomass (lignin) is decomposed in both stages: active and passive pyrolysis stages, without characteristic thermoanalytical peaks. It was found that certain variations in the heat effects can be significantly stimulated by concentration of the three pseudo-components present in samples, which also affects development of theirs decomposition paths. It was established that differences in molecular structures and chemical nature of three pseudo-components in samples should be accounted for dissimilarities observed in the DTG curves. It was concluded that identified variations in appearance in DTG curves are primary related to the variation in percentage of hemicelluloses presented in samples.

2. From volatile release index analysis, it was found that the CB starts to decompose at the lower temperature, while other samples are characterized by very similar initial temperatures (T_{in}). It was established that similar T_{in} values were primarily governed by the content ratio of hemicelluloses, cellulose, and lignin in investigated samples. It was concluded that with an increase in heating rate, devolatilization index (D_i) shows an upward trend, and the more easily the volatiles were released.

3. The MS results showed that H_2, CH_4, H_2O, CO_2 (C_3H_8), CO, and C_2H_6 were the main gaseous products released during the pyrolysis. It was found that majority of gases is generated in the temperature range of 200–500 °C. It was found that H_2O, CO, and CO_2 evolutions arise from lignin source in the biomass, followed by the cellulose, and hemicelluloses. It was found that at the temperatures higher than 450 °C, the H_2 formation can be attributed to secondary pyrolytic reactions. At lower temperatures, the H_2 emission was mainly generated from thermal decomposition of cellulose and hemicelluloses.

4. It was shown that hazelnut shell (HS) could be a good combustion fuel, since during its pyrolysis at high temperature, more gaseous products compared to other systems are very favored and especially generated the high yield of H_2, increasing its energy density. In a

given case, the high temperatures favor higher CO and H_2 production, where the HS can be a very good biomass source for water gas reactions.

References

1. Ohlström M, Mäkinen T, Laurikko J, Pipatti R. New concepts for biofuels in transportation: biomass-based methanol production and reduced emissions in advanced vehicles. VTT Technical Research Centre of Finland; 2001. p. 97.
2. Saxena RC, Adhikari DK, Goyal HB. Biomass-based energy fuel through biochemical routes: a review. Renew Sustain Energy Rev. 2009;13(1):167–78. https://doi.org/10.1016/j.rser.2007.07.011.
3. Maniatis K. Progress in biomass gasification: an overview. In: Bridgwater AV, editor. Progress in thermochemical biomass conversion. London: Blackwell; 2001. pp. 1–31.
4. Faaij A. Modern biomass conversion technologies. Mitig Adapt Strat Glob Change. 2006;11(2):343–75. https://doi.org/10.1007/s11027-005-9004-7.
5. Anwar Z, Gulfraz M, Irshad M. Agro-industrial lignocellulosic biomass a key to unlock the future bio-energy: a brief review. J Radiat Res Appl Sci. 2014;7(2):163–73. https://doi.org/10.1016/j.jrras.2014.02.003.
6. Garcia-Perez M, Lewis T, Kruger C. Methods for producing biochar and advanced biofuels in Washington State. Pullman: Washington State University; 2010. p. 137.
7. Czajczyńska D, Anguilano L, Ghazal H, Krzyżyńska R, Reynolds AJ, Spencer N, Jouhara H. Potential of pyrolysis processes in the waste management sector. Therm Sci Eng Prog. 2017;3:171–97. https://doi.org/10.1016/j.tsep.2017.06.003.
8. Jayaraman K, Gökalp I. Pyrolysis, combustion and gasification characteristics of miscanthus and sewage sludge. Energ Convers Manag. 2015;89:83–91. https://doi.org/10.1016/j.enconman.2014.09.058.
9. Alipour Moghadam R, Yusup S, Azlina W, Nehzati S, Tavasoli A. Investigation on syngas production via biomass conversion through the integration of pyrolysis and air–steam gasification processes. Energ Convers Manag. 2014;87:670–5. https://doi.org/10.1016/j.enconman.2014.07.065.
10. Chaudhari ST, Dalai AK, Bakhshi NN. Production of hydrogen and/or syngas (H_2 + CO) via steam gasification of biomass-derived chars. Energy Fuels. 2003;17(4):1062–7. https://doi.org/10.1021/ef030017d.
11. Boll W, Hochgesand G, Higman C, Supp E, Kalteier P, Müller W-D, Kriebel M, Schlichting H, Tanz H. Gas production, 3. Gas treating. In: Chadwick SS, editor. Ullmann's encyclopedia of industrial chemistry. London: Wiley; 2011.
12. Solid biofuels. Sample preparation. In: BSI British standards.
13. Solid biofuels. Determination of moisture content. Oven dry method. In: BSI British standards.
14. Solid biofuels. Determination of total content of carbon, hydrogen and nitrogen. Instrumental methods. In: BSI British standards.
15. Solid biofuels. Fuel specifications and classes. In: BSI British standards.
16. Solid biofuels. Determination of calorific value. In: BSI British standards.
17. Jianguo X, Zhaolong W. The study of pyrolysis property of pulverized coal by thermogravimetry. J Combust Sci Technol. 1999;5(2):175–9.
18. Inglesby MK, Wood DF, Gray GM. Effect of chemical fractionation treatments on silicon dioxide content and distribution in oryza sativa. In: Stokke DD, Groom LH, editors. Characterization of the cellulosic cell wall. London: Blackwell; 2006. pp. 192–212.
19. Demirbas A. Hydrogen from mosses and algae via pyrolysis and steam gasification. Energy Sour Part A Recovery Util Environ Eff. 2009;32(2):172–9. https://doi.org/10.1080/15567030802464388.
20. Mohan D, Pittman CU, Steele PH. Pyrolysis of wood/biomass for bio-oil: a critical review. Energy Fuels. 2006;20(3):848–89. https://doi.org/10.1021/ef0502397.
21. Gravalos I, Xyradakis P, Kateris D, Gialamas T, Bartzialis D, Giannoulis K. An experimental determination of gross calorific value of different agroforestry species and bio-based industry residues. Nat Resour. 2016;7(01):57.
22. James A, Thring R, Helle S, Ghuman H. Ash management review—applications of biomass bottom ash. Energies. 2012;5(12):3856–73. https://doi.org/10.3390/en5103856.
23. McKendry P. Energy production from biomass (part 1): overview of biomass. Biores Technol. 2002;83(1):37–46. https://doi.org/10.1016/s0960-8524(01)00118-3.
24. Conesa JA, Caballero J, Marcilla A, Font R. Analysis of different kinetic models in the dynamic pyrolysis of cellulose. Thermochim Acta. 1995;254:175–92. https://doi.org/10.1016/0040-6031(94)02102-t.
25. Caballero JA, Conesa JA, Font R, Marcilla A. Pyrolysis kinetics of almond shells and olive stones considering their organic fractions. J Anal Appl Pyrol. 1997;42(2):159–75. https://doi.org/10.1016/s0165-2370(97)00015-6.
26. Slopiecka K, Bartocci P, Fantozzi F. Thermogravimetric analysis and kinetic study of poplar wood pyrolysis. Appl Energy. 2012;97:491–7. https://doi.org/10.1016/j.apenergy.2011.12.056.
27. Yang H, Yan R, Chen H, Lee DH, Zheng C. Characteristics of hemicellulose, cellulose and lignin pyrolysis. Fuel. 2007;86(12–13):1781–8. https://doi.org/10.1016/j.fuel.2006.12.013.
28. Sonobe T, Pipatmanomai S, Worasuwannarak N. Pyrolysis characteristics of Thai-agricultural residues of rice straw, rice husk, and corncob by TG–MS technique and kinetic analysis. In: Proceedings of the 2nd joint international conference on "sustainable energy and environment (SEE'06)"; 2006.
29. Jia C, Chen J, Liang J, Song S, Liu K, Jiang A, Wang Q. Pyrolysis characteristics and kinetic analysis of rich husk. J Therm Anal Calorim. 2019. https://doi.org/10.1007/s10973-019-08366-7.
30. Duan F, Zhang L, Sun X, Huang Y. Comparison of thermal behavior for modified calcium magnesium acetate blended separately with peanutt shell and sewage sludge at different atmospheres. J Therm Anal Calorim. 2017;127(3):2417–25. https://doi.org/10.1007/s10973-016-5829-4.
31. Soncini RM, Means NC, Weiland NT. Co-pyrolysis of low rank coals and biomass: product distributions. Fuel. 2013;112:74–82. https://doi.org/10.1016/j.fuel.2013.04.073.
32. Gómez CJ, Mészáros E, Jakab E, Velo E, Puigjaner L. Thermogravimetry/mass spectrometry study of woody residues and an herbaceous biomass crop using PCA techniques. J Anal Appl Pyrol. 2007;80(2):416–26. https://doi.org/10.1016/j.jaap.2007.05.003.

33. Ghalibaf M, Doddapaneni TRKC, Alén R. Pyrolytic behavior of lignocellulosic-based polysaccharides. J Therm Anal Calorim. 2019;137(1):121–31. https://doi.org/10.1007/s10973-018-7919-y.

34. Özveren U, Özdoğan ZS. Investigation of the slow pyrolysis kinetics of olive oil pomace using thermo-gravimetric analysis coupled with mass spectrometry. Biomass Bioenergy. 2013;58:168–79. https://doi.org/10.1016/j.biombioe.2013.08.011.

35. Jakab E, Faix O, Till F. Thermal decomposition of milled wood lignins studied by thermogravimetry/mass spectrometry. J Anal Appl Pyrol. 1997;40–41:171–86. https://doi.org/10.1016/s0165-2370(97)00046-6.

36. Akalın MK, Karagöz S. Analytical pyrolysis of biomass using gas chromatography coupled to mass spectrometry. TrAC Trends Anal Chem. 2014;61:11–6. https://doi.org/10.1016/j.trac.2014.06.006.

37. Ferdous D, Dalai A, Bej S, Thring R, Bakhshi N. Production of H_2 and medium Btu gas via pyrolysis of lignins in a fixed-bed reactor. Fuel Process Technol. 2001;70(1):9–26.

38. Widyawati M, Church TL, Florin NH, Harris AT. Hydrogen synthesis from biomass pyrolysis with in situ carbon dioxide capture using calcium oxide. Int J Hydrog Energy. 2011;36(8):4800–13. https://doi.org/10.1016/j.ijhydene.2010.11.103.

39. Yang Y, Zhu J, Zhu G, Yang L, Zhu Y. The effect of high temperature on syngas production by immediate pyrolysis of wet sewage sludge with sawdust. J Therm Anal Calorim. 2018;132(3):1783–94. https://doi.org/10.1007/s10973-018-7143-9.

40. Wender I. Reactions of synthesis gas. Fuel Process Technol. 1996;48(3):189–297. https://doi.org/10.1016/s0378-3820(96)01048-x.

41. Duan W, Yu Q. Thermodynamic analysis of hydrogen-enriched syngas generation coupled with in situ CO_2 capture using chemical looping gasification method. J Therm Anal Calorim. 2018;131(2):1671–80. https://doi.org/10.1007/s10973-017-6596-6.

42. Skubiszewska-Zięba J, Charmas B, Kołtowski M, Oleszczuk P. Active carbons from waste biochars. Structural and thermal properties. J Therm Anal Calorim. 2017;130(1):15–24. https://doi.org/10.1007/s10973-017-6143-5.

43. Guo F, Liu Y, Liu Y, Guo C. Catalytic reforming of tar using corncob char and char-supported potassium catalysts. J Therm Anal Calorim. 2017;130(3):1297–306. https://doi.org/10.1007/s10973-017-6420-3.